Special Issue: DTD 2006 in JAPAN
Original Article
J. Jpn. Soc. Microgravity Appl. Vol. 24 No. 3 2007 (231-234)

Study on Characteristics of Thermo-Acoustic Streaming

Kosuke YAMAMOTO[1], Yoshiki YAMAUCHI[1], Takuo KUWAHARA[1] and Mitsuaki TANABE[1]

[1] CST, Nihon University, Chiba, Japan, E-mail : netu336b@yahoo.co.jp

Abstract

"Thermo-acoustic streaming" is a newly-found thermal convection. When heat is released locally in standing sound waves, it is generated toward a node. The driving force of this streaming is considered to be a kind of acoustic radiation force. To clarify the characteristics of this convection, the authors made visualization experiments and numerical simulations. Experiments were done in microgravity to remove the effects of buoyancy. In the simulations, FDTD (Finite Difference Time Domain method) and time-averaged model (ARF model) were used. The heat-source was placed at a node, an anti-node and the middle of the node and the anti-node. The node case, the simulations' results agree with experimental results well. The anti-node and the middle case, however, the ARF results do not agree with the others. Two-dimensional effect, i.e. a flow whose direction is perpendicular to the thermo-acoustic streaming is found. The Rayleigh streaming, the radiation force of 2-D standing sound waves and that of 2-D flow oscillating caused by local heating in the 1-D standing wave were examined as the causes of two-dimensional effect. Analyzing the FDTD, it is concluded that the cause of the flow is the result of the 2-D oscillating flow that occurs near the heat-source.

1. Introduction

Combustion oscillation may occur, when sprayed fuel burn in high-pressure combustors like gas turbines, ramjets and rocket motors. It sometimes yields mechanical or thermal damages to combustors. For example, burning acceleration of droplet combustion was confirmed in standing sound waves of the low frequency of less than 300 Hz [(1)]. In high frequency combustion oscillation (greater than 1000 Hz), it is considered that the oscillation caused by combustion response of acoustic oscillation. It was reported that combustion oscillation may be caused by interference of fuel droplet vaporization and acoustic oscillation in combustors like ramjets and rockets[(2)]. Of particular interest among them is the interference of local heat release and sound.

To clarify the interference, droplet combustion experiments in standing sound waves in microgravity had been made[(3)]. From the experiments, a new thermal convection that is named "thermo-acoustic streaming" was found. As is shown in **Fig. 1**, in the middle of the anti-node and the node , streaming is generated in one direction. At the node and the anti-node, streaming is not generated.

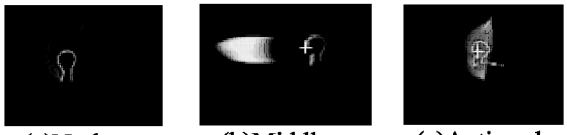

(a)Node (b)Middle (c)Anti-nod

Fig.1 Flame shape at each location

For modeling the streaming, numerical simulations were done[(4),(5)]. Since calculation including burning reaction is complex and requires high computation costs, combustion as a heat source is replaced by a heated wire as a simple model. To clarify whether the simulations give flow field consistent with the experiments, visualization experiments were done[(5)]. The employed visualization method was schlieren method.

2. Theoretical

The driving force of the streaming is considered to be kind of acoustic radiation force. The acoustic radiation force is given by the following equation on the assumption of 1-D acoustic field[(6)].

$$F_R = \left\{ \frac{3(\rho_S - \rho_\infty)}{2\rho_S + \rho_\infty} + 1 - \gamma \right\} V_S \rho_\infty \frac{1}{2} \frac{\partial \overline{u'^2}}{\partial x} \qquad (1)$$

, where $\partial \overline{u'^2} / \partial x$ is the gradient of mean-squared velocity fluctuation. The gradient has the dimension of acceleration as gravity does. ρ_S and V_S are density and volume of heated gas. ρ_∞ is surrounding medium density. γ is the ratio of compressibility. From equation (1), the radiation force is distributed with a half of the wavelength of velocity fluctuation distribution as is shown in **Fig. 2.**

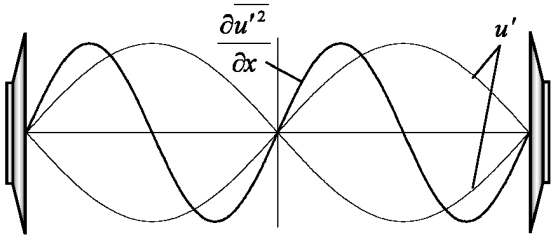

Fig.2 Distribution of velocity fluctuation and gradient of mean-squared velocity fluctuation in 1-D standing sound waves

As is seen in Fig. 2, the gradient reaches the maximum value at the middle of the anti-node and the node. Thus, the force reaches maximum there and disappears at the node and at the anti-node.

Figure 3 shows the direction of acoustic radiation force in standing sound waves. When the gas density

is lower than that of the medium, the gas tries to expand at the anti-node. At the node, it tries to gather, and it is blown toward the node at the middle of the anti-node and the node. The gas whose density is higher than the medium gives just the opposite trends.

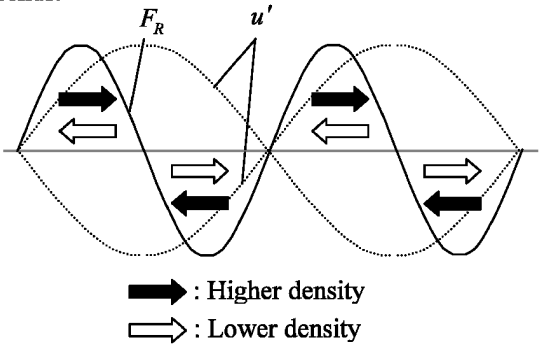

Fig. 3 Direction of the acoustic radiation force

3. Approaches

3.1 Microgravity experiments

Experiments are done in microgravity to remove the effects of buoyancy. Microgravity was realized using the drop shaft of MGLAB (Micro-Gravity Laboratory of Japan). **Figure 4** shows the schematic of the experimental devices.

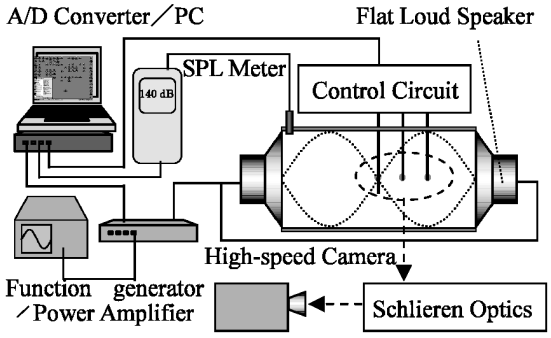

Fig. 4 Schematic of the experimental devices

The hot-wire's temperature is kept constant being controlled by a feed-back circuit. Standing sound waves are generated by two flat loud speakers. The loud speakers are driven in the same phase using a function generator / power amplifier system. Schlieren images are taken using a high-speed camera at a frame rate of 250 1/s. The chamber inner diameter and length are 113 mm and 340 mm. Resonant frequency is 1 kHz to match the condition of high frequency combustion oscillation. SPL (Sound Pressure Level) is 140 dB. The hot-wire is made of pure nickel, whose diameter and length are 0.2 mm and 40 mm, respectively. Temperature is 1000 K. The ambient is air at atmospheric pressure. Ambient temperature is about 290 K.

3.2 Numerical simulation

Among commercial CFD codes, no one models fluid particle oscillation of the wave. Thus, FDTD (Finite Difference Time Domain method) is required. The FDTD is a useful way to analyze the actual phenomenon, but is too inefficient to simulate the oscillating flow, because the time step must be short as sound frequency is high. Therefore, the authors proposed a time-averaged model named as "Acoustic Radiation Force (ARF) model" to improve the computational costs. This model includes the acoustic radiation force as an external force in Navier-Stokes equation. This force is given by the following equation that is obtained from equation (1) on assumption of 1-D standing wave.

$$a = \alpha \frac{\partial \overline{u'^2}}{\partial x} = \alpha \frac{\pi u'^2_{\max}}{\lambda} \sin\left(\frac{4\pi}{\lambda} x\right) \qquad (2)$$

, where α is correction coefficient that is 0.5 in the present case[4], λ is a wavelength of sound, $u'_{\max}$ is the maximum amplitude of velocity fluctuation. The FDTD and the ARF domains are 2-D for simplicity. The computational domain has the same dimension as the chamber. In the FDTD, boundary wall is vibrated horizontally as loud speakers do. Time step of the FDTD and the ARF are 10^{-5} s and 10^{-3} s, respectively. The other conditions are identical with the experiments.

4. Results and Analysis

4.1. Result of experiments and simulations

Figure 5, 6 and 7 show density boundary layer development visualized by the schlieren and those obtained by the FDTD and the ARF. Schlieren images are processed for easy watch. The size of each 25 mm in width and 20 mm in height picture correspond to in actual space.

As is seen in the all three figures, in the case of node, heated air stays at the node. The FDTD results and the ARF results are able to reproduce the reality. But, in the case of middle and anti-node, the ARF fails to reproduce the FDTD results and the experimental results. In the middle case of the FDTD and the experiment, heated air expands vertically soon after heating starts. Shortly after that, it is blown toward the node. In the anti-node case, heated air expands horizontally by the ARF modeling. On the contrary, the FDTD and the experiment show heated air expansion vertically. The vertical flow becomes strong as it approaches to the anti-node from the node. From equation (1) and Fig. 3, it is expected that heated air expands horizontally in the anti-node case and blow only toward the node. The thermo-acoustic streaming seems to accompany an unknown two-dimensional flow.

4.2. Two-dimensional effects

It is considered that the principal cause of the 2-D flow is either "the Rayleigh streaming" or "effect of a radiation force that is generated in 2-D standing sound waves" or "effect of vertical flow oscillation that occurs when the heat source exists in 1-D standing waves". The importances of these three

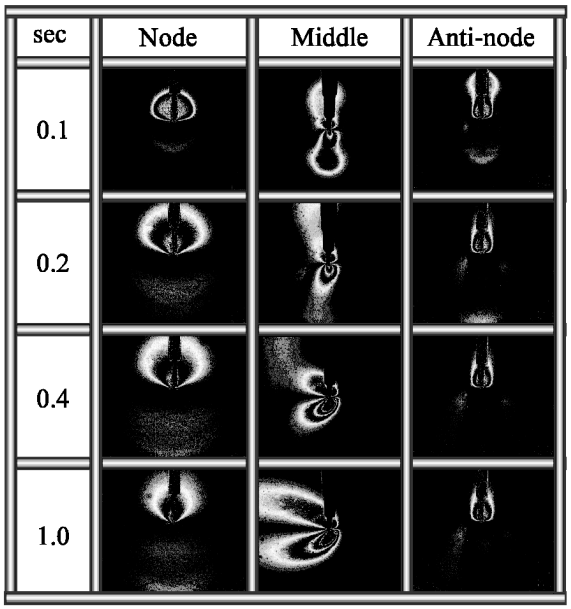

Fig. 5 Density gradient of the schlieren

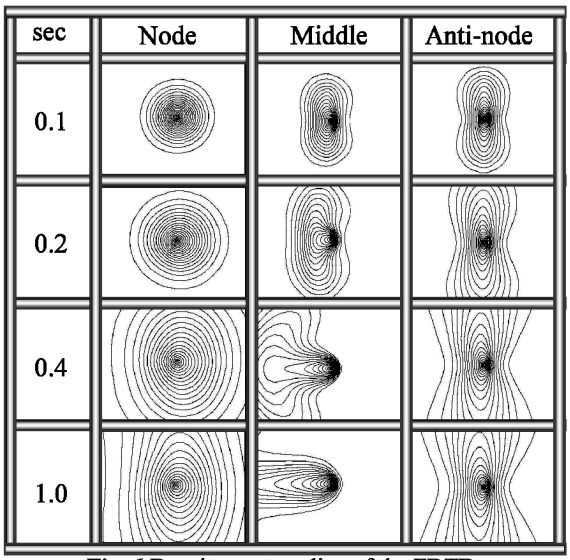

Fig. 6 Density contour line of the FDTD

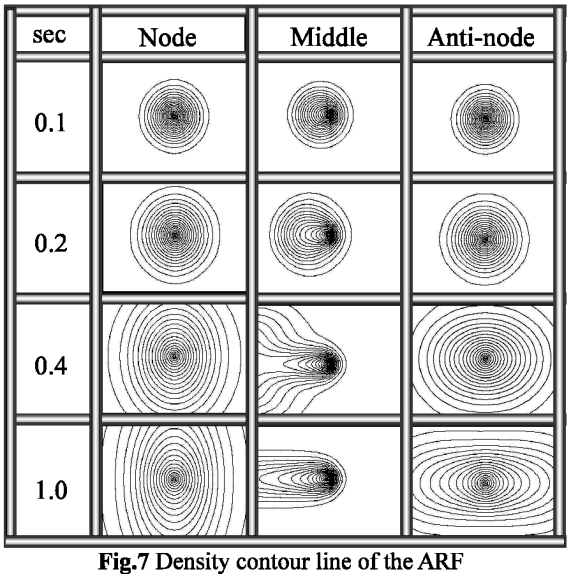

Fig.7 Density contour line of the ARF

are evaluated in the followings.

4.2.1. Effect of the Rayleigh streaming

As is seen in **Fig. 8**, there are parts of standing sound waves (outer area) and oscillating boundary layers (inner area). The Rayleigh streaming that exists in the outer area is stationary circulating flow. At the outer edge of the inner area, there exists steady velocity. It induces the circulating flow in the outer area [7]. The characteristics of 2-D flow described above are explained qualitatively. From analyzing the FDTD results, existence of outer and inner area were confirmed, however, circulating flow was not confirmed clearly. At the anti-node and at the middle of the anti-node and the node, there exists vertical velocity whose magnitude is order of 10^{-4} m/s, that is well below the observed velocity. Thus, the Rayleigh streaming is negligible small.

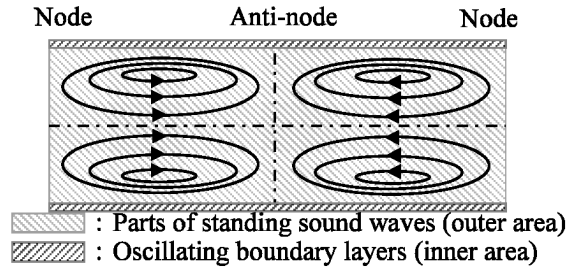

Fig. 8 The Rayleigh streaming

4.2.2. Effect of the 2-D standing sound waves

2-D radiation force that can be generated in 2-D standing sound waves is given by the following equation[8].

$$F = VD\nabla\overline{K_E} + V(1-\gamma)\nabla\overline{P_E} \qquad D = \frac{3(\rho_s - \rho_\infty)}{2\rho_s + \rho_\infty} \tag{3}$$

, where K_E is kinetic energy density, P_E is potential energy density, V is heated gas volume that is assumed to be 10^{-8} m^3 in this case, ρ_s and ρ_∞ are 0.35 and 1.2 kg/m^3 respectively that correspond to air temperature of 1000 and 300 K. **Figure 9** shows distribution of 2-D radiation force that is obtained from equation (3). The same order of amplitude must be applied for vertical and horizontal velocity fluctuations to give the flow circulation shown in the figure. **Figure 10** shows velocity magnitude of the FDTD (1/2 cycle). From analyzing the FDTD, horizontal velocity amplitude is about 0.7 m/s and vertical velocity amplitude is order of 10^{-4} m/s. Thus, acoustic field is almost one dimension at the present system. From Fig. 9, the characteristics of 2-D flow described above are explained qualitatively, while, from Fig. 10, the effect is disregarded quantitatively, because vertical standing waves are not observed.

4.2.3. Effect of the oscillating flow

From analyzing the FDTD, vertical velocity fluctuation, v', near the heat source is found when it is heated. **Figure 11** shows the distribution of the maximum velocity fluctuation at the middle, the anti-node and the node. **Figure 12** shows the

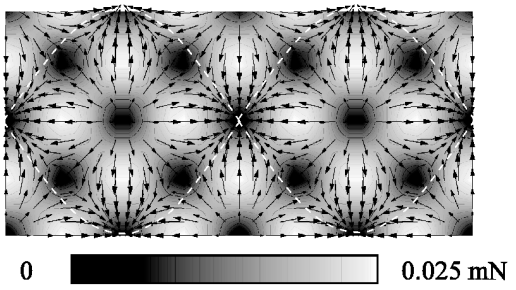

Fig. 9 Distribution of 2-D radiation force

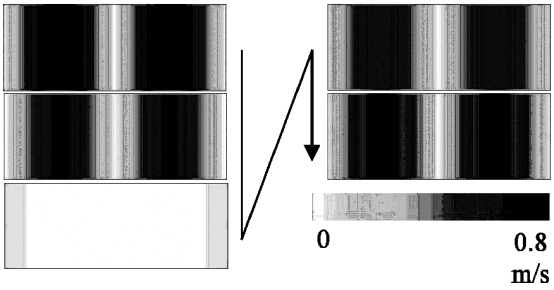

Fig. 10 Velocity magnitude of the FDTD (1/2 cycle)

distribution of the gradient of mean-squared velocity fluctuation at the three case. The ordinate of Fig. 11 expresses the maximum vertical velocity fluctuation v'_{max}. In Fig. 12, the ordinate expresses $\partial\overline{v'^2}/\partial y$. The abscissa of each figures expresses distance from the center of the heat source. Frequency of the v' is twice of the u'. The velocity fluctuation exists not only for solid heat sources but also the case of local fluid heating. Thus, it is considered that the existence of local sharp density difference with rapid expansion generates the vertical velocity fluctuation in standing sound waves.

From Fig. 11, v'_{max} increases with coming close to the anti-node. The amplitude of v' seems to increase with increasing the amplitude of u'. Hence, it is considered that u' causes v'. From Fig.12, $\partial\overline{v'^2}/\partial y$ increases with coming close to the anti-node. It is expected that the vertical streaming gets stronger as u' increases.

In Fig. 11, v'_{max} decreases with increasing distance from the heat source. In Fig. 12, magnitude of $\partial\overline{v'^2}/\partial y$ increases near the heat source. From the previous section, existence of the vertical radiation force due to 2-D standing sound waves was not confirmed clearly. Therefore, it is expected that the 2-D flow is induced by vertical energy dissipation due to the acoustic field disturbed by the heat addition.

5.Conclusions

From analyzing the FDTD, the thermo-acoustic streaming has two-dimensional effect due to 2-D oscillating flow near the heat source.

The gradient of mean-squared vertical velocity

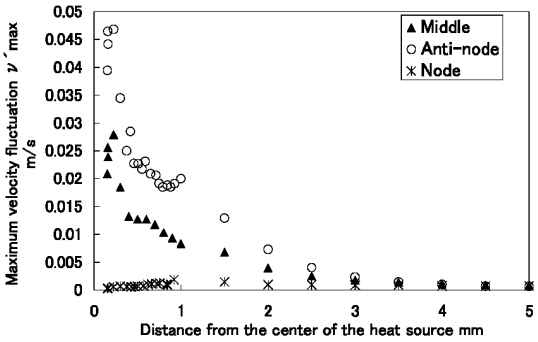

Fig.11 Distribution of the maximum velocity fluctuation v'_{max}

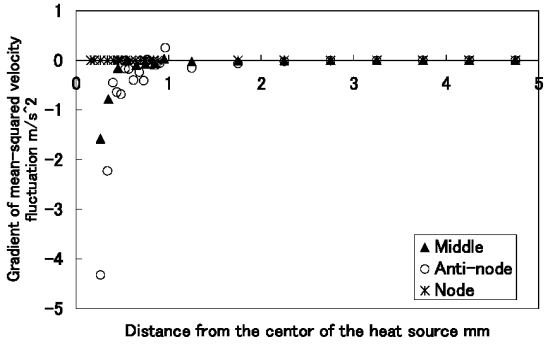

Fig. 12 Distribution of the $\partial\overline{v'^2}/\partial y$

fluctuation exists near the heat source. It is expected that the vertical flow is generated by energy dissipation in vertical direction due to $\partial\overline{p}/\partial y$.

Acknowledgment

This study is carried out as apart of "Ground-based Research Announcement for Space Utilization" promoted by Japan Space Forum.

References

1) Saito, M., Sato, M. and Suzuki, I., *Proceedings of the 31st symposium (Japanese) on combustion,* 549-551, 1993
2) A., Duvvur, C., H., Chaing and W., A., Sirignano, *Journal of Propulsion and Power* ,**12** (2), March-April, .358-365, 1996
3) Tanabe, M., et.al., *Proceedings of the 23rd ISTS,* 2,1662-1668, 2002
4) Tachi, K., et.al., *Journal of the JASMA, 22(1)* 42-46, 2005
5) Yamauchi, Y., et.al., *Proceedings of the 25th ISTS,* 892-897,2006
6) Ultrasonic sound handbook compilation committee, "Ultrasonic sound handbook", Maruzen Press, 162-202, 1999
7) Yano, T., NAGARE, **24**,371-380, 2005
8) Miura, H., *Journal of the ASJ,* **47**(12), 941-947, 1991

Received October 23, 2006
Accepted for publication, July 1, 2007